

PAPER • OPEN ACCESS

## Extreme ultraviolet spectra of multiply charged tungsten ions

To cite this article: Momoe Mita *et al* 2017 *J. Phys.: Conf. Ser.* **875** 012019

View the [article online](#) for updates and enhancements.

### You may also like

- [Study of the charged particle flow near the plasma grid in negative ion source](#)  
S. Masaki, H. Nakano, E. Rattanawongnara et al.
- [Visible transitions of highly charged tungsten ions observed with a compact electron beam ion trap](#)  
Maki Minoshima, Junpei Sakoda, Akihiro Komatsu et al.
- [Evaluation of tungsten influx rate and study of edge tungsten behavior based on the observation of EUV line emissions from  \$W^{3+}\$  ions in HL-2A](#)  
C.F. Dong, S. Morita, Z.Y. Cui et al.



**ECS**  
The  
Electrochemical  
Society  
Advancing solid state &  
electrochemical science & technology

**DISCOVER**  
how sustainability  
intersects with  
electrochemistry & solid  
state science research

# Extreme ultraviolet spectra of multiply charged tungsten ions

Momoe Mita\*, Hiroyuki A. Sakaue<sup>†</sup>, Daiji Kato<sup>†‡</sup>, Izumi Murakami<sup>†‡</sup>,  
and Nobuyuki Nakamura\*

\* Institute for Laser Science, The University of Electro-Communications, Tokyo 182-8585, Japan

<sup>†</sup> National Institute for Fusion Science, Gifu 509-5292, Japan

<sup>‡</sup> Department of Fusion Science, SOKENDAI, Gifu 509-5292, Japan

E-mail: [n.nakamu@ils.uec.ac.jp](mailto:n.nakamu@ils.uec.ac.jp)

**Abstract.** We present extreme ultraviolet spectra of multiply charged tungsten ions observed with an electron beam ion trap. The observed spectra are compared with previous experimental results and theoretical spectra obtained with a collisional radiative model.

## 1. Introduction

Tungsten is the main plasma-facing material in the future experimental fusion reactor ITER, and thus is considered to be the main impurity ions in the ITER plasma [1]. In order to suppress the radiation loss caused by the emission from the impurity tungsten ions, it is important to understand the influx and the charge evolution of tungsten ions in the plasma through spectroscopic diagnostics. There is thus a strong demand for spectroscopic data of tungsten ions. In particular, it has been pointed out that the diagnostics and control of the edge plasma are extremely important for the steady state operation of high-temperature plasmas [2, 3]. Thus the atomic data of relatively low charged tungsten ions are of great significance to the ITER plasma diagnostics [4]. Nevertheless, only few experimental data are available at present. Indeed, no data is available at all for  $W^{8+}$  to  $W^{12+}$  in the atomic spectra database of the National Institute of Standards and Technology (NIST) [5]. For lower charge states, e.g.  $W^{6+}$  and  $W^{7+}$ , experimental data obtained with spark plasma are available for the vacuum ultraviolet to extreme ultraviolet (EUV) region [6, 7, 8]. Recently, observation with an electron beam ion trap (EBIT) has also been done [4, 9]. For higher charge states, e.g.  $W^{13+}$ , several observation using an EBIT have been reported [10, 11, 12] for the EUV region although the identification is still in controversy. In Ref. [11], several lines of  $W^{11+}$  and  $W^{12+}$  are also identified.

In this study, we present EUV spectra of multiply charged tungsten ions observed with an EBIT. Emission lines from  $W^{6+}$  to  $W^{13+}$  are assigned based on electron energy dependence and comparison with previous data. Comparisons with collisional radiative (CR) model calculations are also made.

## 2. Experiment

The present measurements have been performed using a compact EBIT, called CoBIT [13]. It consists essentially of an electron gun, a drift tube, an electron collector, and a high-critical-temperature superconducting magnet. The drift tube is composed of three successive cylindrical



electrodes that act as an ion trap by applying a positive potential (typically 30 V) at both ends with respect to the middle electrode. The electron beam emitted from the electron gun is accelerated towards the drift tube while it is compressed by the axial magnetic field (typically  $\sim 0.08$  T) produced by the magnet surrounding the drift tube. The compressed high-density electron beam ionizes the ions trapped in the drift tube. The space charge potential of the compressed electron beam also acts as radial ion trap. In the present study, a vapor of  $\text{W}(\text{CO})_6$  was introduced into the trap through a gas injector for producing and trapping tungsten ions. To produce tungsten ions with charge states  $q = 6 - 13$ , the electron energy was changed from 100 to 280 eV by changing the electron gun (cathode) potential while the middle of the drift tube was kept at the ground potential. The electron beam current was 3 to 7.5 mA depending on the electron energy. EUV emission from the trapped tungsten ions was observed with a grazing-incidence flat-field spectrometer [14] consisting of a 1200 g/mm concave grating (Hitachi 001-0660) and a Peltier-cooled back-illuminated CCD (Roper PIXIS-XO: 400B). The wavelength calibration has been preliminary done with the previously observed lines of Er-like  $\text{W}^{6+}$  [6] and Pm-like  $\text{W}^{13+}$  [12].

### 3. Collisional radiative model calculation

We made collisional radiative (CR) model calculation to simulate the experimental spectra for  $\text{W}^{6+}$  to  $\text{W}^{8+}$ . In the calculation, excited-level populations were obtained by solving quasi-stationary-state rate equations that account for electron collisions (excitation, deexcitation, and ionization) and radiative decays (E1, E2, E3, M1, and M2). The collision strengths, decay rates, and energy levels were calculated with the HULLAC code (v9.601) [15] based on fully relativistic wave functions and the distorted-wave approximation. For each charge state, all the possible  $5s^25p^k4f^m$ ,  $5s^25p^{k'}4f^{m'}nl$ ,  $5s5p^{k''}4f^{m''}$  and  $5s5p^k4f^mnl$  configurations ( $k+m = k'+m'+1 = k''+m''-1$ ) with  $n \leq 6$  and  $l \leq 4$  were taken into account. The number of the levels are 281, 2,527, and 15,248 for  $\text{W}^{6+}$ ,  $\text{W}^{7+}$ , and  $\text{W}^{8+}$ , respectively.

### 4. Results and discussion

Figure 1 shows the EUV spectra obtained at electron beam acceleration voltages of 100 to 280 V. For simplicity, here we refer to the acceleration voltage (multiplied by the elementary charge) as “electron energy” although the actual electron energy is generally lower than the acceleration voltage by few to few tens of eV. From the comparison with the previous observations [4, 6], emission lines at 21.6 and 26.1 nm observed at 90 eV can be identified to be  $5p_{1/2} - 5d_{3/2}$  and  $5p_{3/2} - 5d_{5/2}$  lines in  $\text{W}^{6+}$ , respectively. The features observed at around 20 nm in the 115 eV spectrum (the lines indicated by the square bracket) are consistent with those observed in the spectra obtained by Clementson *et al.* with the Livermore EBIT [4], and thus can be assigned to  $5p - 5d$  and  $5p - 6s$  lines from  $\text{W}^{7+}$  by following their identification.

When the energy was increased from 115 to 130 eV, the  $\text{W}^{7+}$  features almost disappeared, whereas the features at around 19.5 nm (the lines indicated by the square bracket in the 130 eV spectrum) remained. We thus assign these lines to  $\text{W}^{8+}$ . By further increasing the electron energy to 150 eV, the  $\text{W}^{8+}$  lines almost disappeared, and the four lines indicated by the arrows appeared; thus we assign these four lines to  $\text{W}^{9+}$ . In a similar way, the observed lines in the 190 - 280 eV spectra can be assigned to  $\text{W}^{10+}$  to  $\text{W}^{13+}$  step by step as shown in the figure. The spectra of  $\text{W}^{12+}$  and  $\text{W}^{13+}$  are consistent with our previous observation [12], which may confirm the validity of our present and previous assignment.

It may be noted that noticeable differences can be found between the present spectra and the Livermore EBIT spectra [4] especially for the electron energies of above 150 eV. We consider the differences are due to the different experimental conditions (probably different amount of injected  $\text{W}(\text{CO})_6$ ) that led to a higher and narrower charge state distribution for the present case.

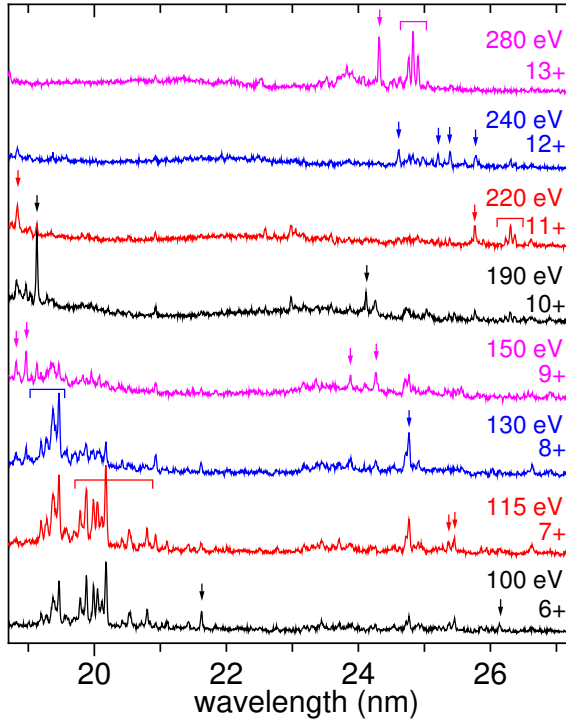


**Figure 1.** EUV spectra of multiply charged tungsten ions obtained with a compact electron beam ion trap. The electron energy at which each spectrum was obtained is shown in the right side. The lines indicated by the arrows or the brackets in each spectrum are assigned to the charge state written in the right side based on the energy dependence and the comparison with previous studies [4, 12].

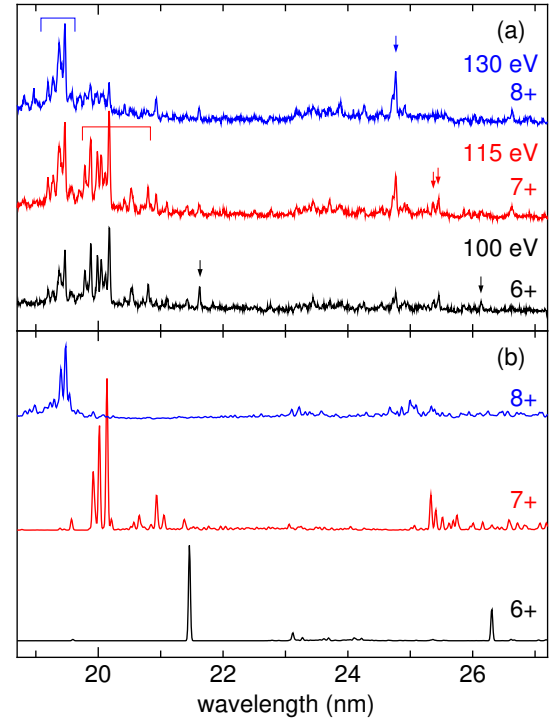


**Figure 2.** Comparison between the experimental and model spectra. (a) Experimental spectra (same as the bottom three spectra of Fig. 1). (b) CR model spectra obtained for electron energies of 100 eV (6+), 115 eV (7+), and 130 eV (8+) with an electron density of  $10^{10} \text{ cm}^{-3}$ . Note that the wavelength scale of the model spectra is shifted to fit the experimental spectra (see text).

Figure 2 shows comparisons between the experimental and CR model spectra for  $\text{W}^{6+}$  to  $\text{W}^{8+}$ . The model spectra were calculated for electron energies of 100 eV (6+), 115 eV (7+), and 130 eV (8+) and an electron density of  $10^{10} \text{ cm}^{-3}$ . Unfortunately, since the accuracy of the calculated wavelength is poor, the model spectra are shifted to longer wavelength direction by 1 nm for 6+, 1.65 nm for 7+, and 1.05 nm for 8+ to fit the experimental spectra. Other than the transition wavelength, the experimental spectral features are generally well reproduced by the model as seen in the figure.

The two prominent peaks in the  $\text{W}^{6+}$  model spectrum are  $5p_{1/2} - 5d_{3/2}$  and  $5p_{3/2} - 5d_{5/2}$  transitions, which are consistent with the identification in the previous Livermore EBIT observation [4]. The two lines are also confirmed in our present spectrum obtained at an electron energy of 100 eV.

Several lines at around 20 nm (shifted wavelength) in the  $\text{W}^{7+}$  model spectrum are  $4f^{13}5p_{1/2} - 4f^{13}5d_{3/2}$  transitions. On the other hand, according to Clementson *et al.* [4] and Ryabtsev *et al.* [16], the cluster of lines observed at around 20 nm contains not only  $5p - 5d$  transitions but also  $5p - 6s$  transitions. We have no idea at present about the absence of the  $5p - 6s$  transitions in the model spectrum. We have also assigned two lines indicated by the arrows at around 25.5 nm in the 115 eV spectrum to  $\text{W}^{7+}$ . They may correspond to  $5p_{3/2} - 5d_{5/2}$

transitions predicted at around 25.3 nm (shifted wavelength) in the  $W^{7+}$  model spectrum.

The cluster of lines at around 19.5 nm (shifted wavelength) in the  $W^{8+}$  model spectrum consists of  $5p - 5d$  and  $4f - 5d$  transitions, which should correspond to the observed cluster of lines indicated by the bracket in the 130 eV spectra. As seen in the figure, the experimental spectral features are well reproduced by the model. The peak at 24.8 nm in the experimental spectrum has also been assigned to  $W^{8+}$ , which may correspond to  $5p_{3/2} - 5d_{5/2}$  transitions appeared at around 25 nm (shifted wavelength) in the  $W^{8+}$  model spectrum.

The present identification seems to be inconsistent with the ionization energy values [17] because  $W^{7+}$  (122 eV required) and  $W^{8+}$  (141 eV required) lines are assigned in the spectrum at an electron energy of 100 eV. The similar inconsistency is also found in the previous Livermore EBIT spectra, where they observed  $W^{6+}$  (65 eV required) lines at 43 eV and  $W^{7+}$  (122 eV required) lines at 72 eV. Ionization from metastable excited states [18, 19] may account for this inconsistency. Indeed, our CR model calculations on  $W^{6+}$  and  $W^{7+}$  indicate that the metastable states with an energy of  $\sim 40$  eV can have a population comparable with or even larger than that of the ground state. The ionization from such metastable states can make the ionization threshold lower by  $\sim 40$  eV, which may account for the experimental energy dependence.

## 5. Summary and outlook

We have observed EUV spectra of multiply charged tungsten ions  $W^{6+}$  to  $W^{13+}$  using a compact electron beam ion trap. Based on the electron energy dependence and the comparison with existing data, charge state has been assigned for the observed lines. The CR model calculations have also been done and compared with the present and previous experimental data. Although the model is found to reproduce the general features of the experimental spectra, there are still some discrepancies. The CR model results strongly depend on the potential optimization and the configurations taken into account; thus further detailed analysis are needed and in progress. Observations for other wavelength regions and the CR model calculations for other charge states are also in progress, and will be published elsewhere.

## Acknowledgements

This work was supported by JSPS KAKENHI Grant Numbers 16H04623, 16H04028, and partly supported by the JSPS-NRF-NSFC A3 Foresight Program in the field of Plasma Physics (NSFC: No.11261140328, NRF: No.2012K2A2A6000443) and the NIFS Collaboration Research program (NIFS17KLPP058).

## References

- [1] Ralchenko Y 2013 *Plasma Fusion Res.* **8** 2503024
- [2] Janev R K (ed) 1995 *Atomic and Molecular Processes in Fusion Edge Plasmas* (New York: Springer)
- [3] Matt S, Fiegele T, Senn G, Becker K, Deutsch H, Echt O, Stamatovic A, Scheier P and Märk T 2001 *Atomic and Plasma-Material Interaction Data for Fusion*, IAEA **9** 11
- [4] Clementson J, Lennartsson T and Beiersdorfer P 2015 *Atoms* **3** 407
- [5] Kramida A, Yu Ralchenko, Reader J and NIST ASD Team 2015 NIST Atomic Spectra Database (ver. 5.3), [Online]. Available: <http://physics.nist.gov/asd> [2017, July 6]. National Institute of Standards and Technology, Gaithersburg, MD.
- [6] Sugar J and Kaufman V 1975 *Physical Review A* **12** 994
- [7] Wyart J F, Kaufman V and Sugar J 1981 *Physica Scripta* **23** 1069
- [8] Ryabtsev A, Kononov E, Kildiyarova R, Tchang-Brillet W Ü L, Wyart J F, Champion N and Blaess C 2015 *Atoms* **3** 273
- [9] Mita M, Sakaue H A, Kato D, Murakami I and Nakamura N 2017 *Atoms* **5** 13
- [10] Hutton R, Zou Y, Almandos J R, Biederman C, Radtke R, Greier A and Neu R 2003 *Nucl. Instrum. Methods B* **205** 114–118
- [11] Li W, Shi Z, Yang Y, Xiao J, Brage T, Hutton R and Zou Y 2015 *Phys. Rev. A* **91**(6) 062501

- [12] Kobayashi Y, Kubota K, Omote K, Komatsu A, Sakoda J, Minoshima M, Kato D, Li J, Sakaue H A, Murakami I *et al.* 2015 *Physical Review A* **92** 022510
- [13] Nakamura N, Kikuchi H, Sakaue H A and Watanabe T 2008 *Rev. Sci. Instrum.* **79** 063104
- [14] Ohashi H, Yatsurugi J, Sakaue H A and Nakamura N 2011 *Rev. Sci. Instrum.* **82** 083103
- [15] Bar-Shalom A, Klapisch M and Oreg J 2001 *J. Quant. Spectrosc. Radiat. Trans.* **71** 169
- [16] Ryabtsev A, Kononov E Y, Kildiyarova R, Tchang-Brillet W Ü L and Wyart J 2013 *Physica Scripta* **87** 045303
- [17] Kramida A E and Shirai T 2009 *At. Data Nucl. Data Tables* **95** 305
- [18] Sakoda J, Komatsu A, Kikuchi H and Nakamura N 2011 *Phys. Scr.* **T144** 014011
- [19] Windberger A, Torretti F, Borschevsky A, Ryabtsev A, Dobrodey S, Bekker H, Eliav E, Kaldor U, Ubachs W, Hoekstra R, Crespo López-Urrutia J R and Versolato O O 2016 *Phys. Rev. A* **94**(1) 012506